

RESEARCH

Open Access



Neuropeptide S and its receptor aggravated asthma via TFEB dependent autophagy in bronchial epithelial cells

Zhixu Wang^{1,2†}, Peng Zhao^{1,2†}, Gen Yan^{3†}, Aijuan Sun^{5,6†}, Li Xu^{1,2}, Jiao Li^{1,2}, Xiaorun Zhai^{1,2}, Xiangcen Liu^{1,2}, Tingting Mei^{1,2}, Yinghua Xuan⁴ and Yunjuan Nie^{1,2*}

Abstract

Background Asthma is a prevalent respiratory disorder with limited treatment strategy. Neuropeptide S (NPS) is a highly conserved peptide via binding to its receptor NPSR, a susceptibility gene for asthma from genomics studies. However, little is known about the role of NPS-NPSR in the pathogenesis of asthma. This study was performed to determine the effect and underlying mechanism of NPS-NPSR on asthma.

Methods NPSR knockdown was verified to affect asthma through autophagy by transcriptome sequencing and molecular biology experiments in animal models. Silencing of transcription factor EB in a bronchial epithelial cell line and validation of NPS-NPSR activation of autophagy dependent on transcription factor EB.

Results Our results showed that NPSR expression was markedly increased in asthmatic humans and mice, mainly localized in bronchial epithelial cells. Using ovalbumin (OVA) and papain-induced asthma mouse models, NPSR-deficient mice exhibited significantly alleviated asthma, with reduced small airway lesions and inflammatory infiltration compared with wild-type mice. OVA and papain promoted TFEB-mediated autophagy with increased ATG5 and LC3 II expression, and NPS effectively regulated the activation of TFEB and autophagy. In turn, specific TFEB knockdown could restore the effect of exogenous NPS and its receptor antagonist on the autophagy and cytokines secretion in bronchial epithelial cells. Furthermore, Prkcg may be the key upstream targeting of the TFEB-autophagy pathway involved in asthma.

Conclusions NPS-NPSR exacerbated asthma by regulating the TFEB-autophagy axis in airway epithelial injury, which may be a potential target for asthma therapy.

Keywords Neuropeptide S, Asthma, Bronchial epithelial cell, Autophagy, TFEB

[†]Zhixu Wang, Peng Zhao, Gen Yan and Aijuan Sun contributed equally to this work.

*Correspondence:

Yunjuan Nie

nieyunjuan@jiangnan.edu.cn

¹ Department of Basic Medicine, Wuxi School of Medicine, Jiangnan University, Wuxi 214122, China

² MOE Medical Basic Research Innovation Center for Gut Microbiota and Chronic Diseases, School of Medicine, Jiangnan University, Wuxi 214122, China

³ Department of Radiology, The Second Affiliated Hospital of Xiamen Medical College, Xiamen 361000, China

⁴ Department of Microbiology and Immunology, Xiamen Medical College, Xiamen 361023, Fujian, China

⁵ Department of Oncology, The Second Affiliated Hospital of Soochow University, Suzhou 215004, China

⁶ Department of Pathology, Affiliated Wuxi People's Hospital of Nanjing Medical University, Wuxi Medical Center of Nanjing Medical University, Wuxi People's Hospital, Wuxi 214023, Jiangsu, China



Introduction

Asthma is a complex respiratory disease characterized by bronchial hyperresponsiveness, variable airflow obstruction, and airway inflammation. The prevalence of asthma has been increasing and affects over 300 million people, entailing a heavy socioeconomic burden [1]. Multiple elements have been proposed to contribute to asthma pathogenesis, including genetic factors, immunologic response, environmental and pharmacologic mediation [2, 3]. Hence, there are heterogeneous phenotypes, with the underlying pathogenetic mechanisms poorly understood. It is urgent to identify crucial pathways involved in asthma and guide the development of therapeutic targets effectively [2].

Respiratory epithelial cells (ECs) are the first defense barrier against exposure to stimuli such as pathogens, pollutants, allergens, and even the lung microbiome. It has been well recognized that ECs play a vital role in prompting asthma [4]. Many of the identified susceptibility genes for asthma, such as MUC5AC (Mucin 5AC), IL33 (Interleukin 33), IL1R1 (Interleukin 1 Receptor Type 1), and TSLP (Thymic Stromal Lymphopoietin), are predominantly expressed by epithelial cells [5]. In turn, dysfunction of the epithelial barrier has been identified to increase allergen inhalation [6], with more release of typical TH2 cytokines, resulting in significant respiratory inflammation and airway remodeling contributing to the pathogenesis of asthma [7]. Therefore, ECs have emerged as a major driver of asthma development. The respiratory tract is anatomically divided into the upper and lower respiratory tracts. The upper respiratory tract includes the nasal cavity, pharynx, and larynx, while the lower respiratory tract comprises the conducting airways (trachea, bronchi, and bronchioles) and the respiratory zones (respiratory bronchioles and alveoli) [8, 9]. The epithelial cells lining the respiratory tract differ in type and function depending on their anatomical location. Among these, bronchial epithelial cells are particularly critical for investigation in the context of asthma [10, 11].

Autophagy is a highly conserved metabolic process in which abnormal proteins and impaired organelles are delivered and degraded in the lysosome [12]. As a major cellular quality control mechanism, autophagy has been shown to play important roles in inflammatory response, cytokine secretion, and airway remodeling, thereby promoting or aggravating various inflammatory lung diseases [13, 14]. Recently, autophagy-related genes, including ULK1 (Unc-51 Like Autophagy Activating Kinase 1), MAPLC3B (Microtubule Associated Protein 1 Light Chain 3 Beta), Beclin-1, and Atg5 (Autophagy Related 5), have been identified as being involved in various types of asthma [14–16]. For example, Atg5 expression in patients with asthma is higher in lungs of asthma

patients and mice models compared with normal lungs [17]; the overexpression of autophagy-related genes impairs bronchial epithelial function in asthma [14, 15]; and IL-13 (Interleukin 13) activates autophagy in differentiated human tracheal airway epithelial cells to direct mucin secretion and cell oxidant stress responses [18, 19]. These findings suggest an important direction for asthma treatment via targeting the autophagy process. However, the mechanism of promoting autophagy during the progression of asthma has not been completely understood.

Neuropeptide S (NPS) is a highly conserved peptide found in all tetrapods that is secreted by neuroendocrine cells. Via its G protein-coupled cell surface receptor Neuropeptide S Receptor 1 (NPSR1), NPS plays important roles in multiple neuroendocrine, behavioral, and inflammatory responses [20, 21]. NPSR1 was uncovered as a susceptibility gene for asthma and related traits by positional cloning. Moreover, the correlation of NPSR1 single nucleotide polymorphisms (SNPs) with asthma has been replicated in ethnically diverse populations [22–24], and supported by a large-scale genome-wide association study (GWAS) [25]. Recently, elevated expression of NPS and its receptor in airways, lung tissue, and alveolar lavage fluid of asthmatics was found, while in blood and sputum cells, large monocytes/macrophages and eosinophils were identified as NPSR-positive cells [26, 27]. However, the specific function and underlying mechanism of NPS-NPSR system on asthma remain unclear.

In this study, we investigated the effects of NPS-NPSR in mice models of asthma, showing that aberrant autophagy in epithelial cells controlled by NPS-NPSR axis contributed to the progression of OVA and papain-induced asthma. We also provided the molecular mechanism involved in this autophagy process. The present study provides novel therapeutic targets for controlling asthma.

Material and methods

Animals

C57BL/6 mice were purchased from Spearfish (Beijing) Biotechnology Co. NPSR-deficient mice (C57BL/6)-Npsr1em1Cya) were purchased from Sayer (Suzhou) Biotechnology Co. Each cage of 5 mice was housed under specific pathogen-free conditions in a climate-controlled room (25 °C, 55% humidity, 12 h light/dark cycle). Procedures involving mice were approved by the JNU Animal Care and Use Teaching Committee (JN. No20230830m0880315 [350], approval date 8/30/2023).

Reagents

OVA (A5253) was obtained from Sigma-Aldrich; Papain (T19503) was purchased from Taojitsu; Alum Injection

Adjuvant (77161) was purchased from Thermo Fisher Scientific; Anti-NPSR Antibody (orb158023) was purchased from biorbyt; Anti-Ep-CAM Antibody (G8.8): sc-53532; Anti-ATG5 antibody (#12994), anti-LC3B antibody (#3868S), anti-Beclin-1 antibody (#3495 T), anti-P62 antibody (#23214S) were purchased from Cell Signaling Technology (Danvers, MA, USA), β -actin (#21338) was purchased from Signalway Antibody (College Park City, MD, USA). Anti-TFEB antibody #41488 and anti-PRKCG antibody #55375 were from Signalway Antibody, and flow cytometry antibodies, including FITC anti-mouse CD170 (Siglec-F) Antibody (S17007L) and PE anti-mouse CD11c (N418) from Biolegend and ThermoFisher, respectively. BCA protein detection kit (P0012S) and DAPI (C1002) were provided by Beyotime.

Animal models

In the OVA-induced asthma model, we used 6–8 weeks old female mice. As previously reported [28–30], on days 0 and days 10, we sensitized with Imject Alum adjuvant 2 mg demulsified OVA 75 μ g intraperitoneally and ensured that the total volume injected was 200 μ l. Under isoflurane anesthesia, mice were given OVA (50 μ g in 40 μ l PBS) intraductally on days 21, 22, and 23, respectively. Mice were necropsied on day 25, and peripheral blood, BALF (Bronchoalveolar Lavage Fluid), and lung tissue were collected for further study. In the papain model, we administered papain (30 μ g in 40 μ l PBS) intratracheally to female mice (6–8 weeks) continuously on days 0, 1, and 2 for 3 days and executed them on day 7.

Bronchoalveolar lavage fluid collection and analysis

The lungs were lavaged twice with 1 ml of sterile PBS, and bronchial lavage fluid was collected from the asthma model and control mice. 4 °C and 500 g for 5 min were resuspended in PBS and counted, and the supernatant was assayed for protein concentration using the BCA protein assay kit.

Lung histological assay

Lung tissues (left lower lobe) were fixed with 4% paraformaldehyde, dehydrated and embedded in paraffin, and subsequently cut into 4- μ m sections. Lung tissue sections were stained with hematoxylin and eosin staining (H&E) and Periodic Acid-Schiff stain (PAS) to evaluate the inflammation and mucin levels in the bronchi.

Flow cytometry assay and cell sorting

Cells were obtained from BALF, lysed for erythrocytes, and centrifuged and resuspended for surface staining by incubation with flow antibodies anti-mouse CD11c and anti-mouse Siglec-F antibodies for 30 min at 4 °C. Cells with low CD11c and high Siglec-F expression were then

sorted by flow cytometry (BD & FACS Aria III). Each cell lineage was identified as follows: Eosinophils (Eos), CD11c-Siglec-F+.

Cell culture and transfection

BEAS-2B cells (XY Biotechnology, China) were maintained at 37 °C in an atmosphere of 5% CO₂ and 95% relative humidity, using DMEM supplemented with 10% fetal bovine serum (FBS, Gibco, USA). Transfection of BEAS-2B cells with small interfering RNA targeting TFEB (siTFEB) was performed using Lipofectamine 2000 (Thermo Fisher Scientific). The siTFEB sequence was as follows: sense strand: GACGAAGGUUCAACAUCAATT; antisense strand: UUGAUGUUUGAACCUUCGUCTT. After 24 h of routine culture, an asthma cell model was induced by treating the cells with ovalbumin (OVA, 5 mg/ml) at 37 °C for 24 h to facilitate subsequent experiments [31].

RNA isolation and sequencing

Total RNA was isolated from lung tissues and BEAS-2B cells using TRIzol reagent (Vazyme Biotech Co., Ltd, Nanjing, China). cDNA was prepared using Hifair® III 1st Strand cDNA Synthesis SuperMix (11137ES60, Yeasen Biotechnology) to prepare cDNA. Real-time fluorescent quantitative PCR of target genes was detected by qPCR syber GREEN (11201ES08, Yeasen Biotechnology) on a LightCycler®480 PCR detection system (AXYP-CR96LC480 WNF, Roche, Foster City, CA, USA). mRNA expression. The primer sequences were as Table 1. Relative mRNA expression levels were calculated using the $2^{-\Delta\Delta C_t}$ method, with GAPDH serving as the internal reference.

Isolation of nuclear and cytoplasmic proteins

Nuclear and cytoplasmic proteins from cultured cells were obtained using the Nuclear and Cytoplasmic Protein Extraction Kit (P0027).

Western blotting

Total protein was extracted from lung tissue or treated BEAS-2B cells with 1×RIPA lysate and then centrifuged at 4 °C for 15 min at 12,000 rpm to collect the supernatant. We then determined its protein concentration using a BCA protein assay kit (Biyuntian Biotechnology, Shanghai, China). Equal amounts of protein (30 μ g) were injected in 10% and 12% SDS-PAGE gels and transferred to nitrocellulose membranes. After being blocked with 5% BSA for 1 h at room temperature, the proteins were incubated with the target primary antibody (1:1000) overnight at 4 °C and with the HRP-labeled secondary antibody (1:10,000) for 1 h at room temperature and then visualized with the ECL kit (Millipore, Billerica, MA,

Table 1 Primer sequences

Primer	Forward (5'-3')	Reverse (5'-3')
NPS (mouse)	GGCTCGTTAAACTCAGCTTCG	GGAAGAGAGGACCCGGATAACA
NPSR1 (mouse)	GTGCCGATGCTAGATTCTTC	CAGGACCCACAGGGTTATCAG
IL-4 (mouse)	GGTCTCAACCCCCAGCTAGT	GCCGATGATCTCTCTCAAGTGAT
IL-5 (mouse)	GCAATGAGACGATGAGGCTTC	GCCCTGAAAGATTTCTCCAATG
IL-13 (mouse)	TGAGCAACATCACACAAGACC	GGCCTTGCGGTTACAGAGG
TSLP (mouse)	GGAGATTTGAAAGGGGCTAAG	TGGGCAGTGGTCATTGAG
MUC5AC (mouse)	GGAACCCGTGTGTACTCAT	GGTGCACCGTACATTTCTGC
IL-25 (human)	ATGTACCAGGTGGTTGCATTC	TGCTGTTGAGGGGTCCATCT
TFEB (human)	GACGAAGGUUCAACAUAATT	UUGAUGUUGAACCUUCGUCTT
Prkcg (human)	AGATCCATATTACTGTTGGCGA	TCAGTTTCACGTAGGGATCAG
TSLP (human)	GGGCTGGTGTAACTTACGACTTCA	ACTCGGTACTTTTGGTCCCACTCA
IL-33 (human)	TGAATCAGGTGACGGTGTGATGG	TGAAGGACAAAGAAGGCCTGGTC
NPSR1 (human)	ATGCCAGCCAACCTCACAGAG	AAGGAGTAGTAGAAGGAACCCC
NPS (human)	AATCTCATCTAGTTCTGTCGCT	CTCTGTCCAATCTGGTTGGG
GAPDH (mouse)	CCTCCGTTGCTCTACC	CAACCTGGTCTCAGTGTA
GAPDH (human)	TGTGGGCATCAATGGATTGG	ACACCATGTATTCCGGGTCAAT

USA) using the ChemiDoc MP imaging system (Bio-Rad Laboratories, Hercules, CA, USA). Bands were quantified using ImageJ software (ImageJ-Java 1.8.0_172 (164 bits), Software Inquiry; Quebec, QC, Canada). Protein band intensities were quantified using densitometry analysis. Integrated density values of target bands were normalized to corresponding loading controls, with background subtraction applied. Relative expression levels were calculated and statistically analyzed to assess differences between experimental groups.

Immunofluorescence assay

For lung tissue sections, after deparaffinization and antigen repair, the sections were incubated with 5% donkey serum for 1 h at room temperature, followed by the addition of a primary antibody and incubation at 4 °C overnight. After three washes with PBS, the sections were incubated at 37 °C for 1 h with secondary antibodies protected from light. After three washes with PBS, the sections were sealed with a sealer containing DAPI and visualized under the Zeiss confocal microscope. Beas-2b cells (2×10^4 /well) were spread in 48-well plates containing coverslips and treated with the indicated treatments. Then, cells were fixed in 4% paraformaldehyde for 10 min and permeabilized with 0.1% Triton X-100 (Sigma Aldrich, Shanghai, China). After blocking with 5% BSA for 30 min, the cells were incubated with the target primary antibody at 4 °C overnight. After removal of the primary antibody and three washes with PBS, the cells were further incubated with Alexa 488-labeled secondary antibody (CST, Danvers, MA, USA) and DAPI (4,6-diamidino-2-phenylindole) for 2 h (2.5 µg/ml) for 5 min. The

coverslips were then transferred to glass substrates and photographed under a laser-scanning confocal fluorescence microscope. Fluorescence intensity was quantified by measuring the mean pixel intensity of regions of interest (ROIs) corresponding to target signals. Background intensity was subtracted, and normalized values were statistically analyzed to compare expression levels across experimental groups.

Statistical analysis

GraphPad Prism 9 is used to assess normality, variability, and statistical analysis of data sets. Data are expressed as mean \pm SEM. In vitro data were from at least three independent experiments, and in vivo data were from experiments with 6–8 mice per group. Statistical analyses were performed using t-test, one-way ANOVA, two-way ANOVA, and Tukey's multiple comparison test. The level of significance $p < 0.05$ was considered statistically significant. Statistical significance was defined as * $p < 0.05$, ** $p < 0.01$, and *** $p < 0.001$.

Results

NPS and its receptor NPSR are overexpressed in asthma disease

We firstly performed mouse models using OVA and papain to evaluate the expression of NPSR in asthmatic mice compared to normal mice (Fig. 1A). Hematoxylin and eosin (H&E) staining revealed increased inflammation and bronchial thickening in the trachea of mice treated with OVA or papain (Fig. 1B). Additionally, cell counts and protein assays from alveolar lavage fluid, along with the relative mRNA expression levels of

inflammatory factors in lung tissue, further confirmed the successful establishment of the asthma mouse model (Fig. 1C–E). The results showed that both mRNA and protein levels of NPS-NPSR were increased in the lung tissues of asthmatic mice (Fig. 1F–I). Immunohistochemical staining exhibited strong positivity for NPSR in lungs of OVA and papain induced mice (Fig. 1J). Interestingly, all NPSR-positive expression seemed to localize in the bronchi's epithelial cells. The overexpression of NPSR in bronchi's epithelial cells was further determined by double-label immunofluorescence assay against NPSR and epithelial cell marker Ep-CAM (Fig. 1K). These results suggest that NPS-NPSR in bronchial epithelial cells may be involved in the development of asthma. Meanwhile, we analyzed the dataset GSE37693 from the GEO database and found higher NPSR mRNA level in IL-13-stimulated human primary airway epithelial cells (Fig. 1L, M). All these phenomena reveal that NPS-NPSR activation is closely related to asthma.

NPSR knockout relieves asthma and airway inflammation

To determine the role of NPSR on asthma, we generated NPSR knockout mice and constructed OVA and papain induced asthma models. Although NPSR knockout mice were identified through genetic screening, we further verified the knockout efficiency in lung tissues to ensure experimental consistency. Specifically, we analyzed the relative expression levels of NPSR protein and mRNA in lung tissues of NPSR knockout and non-knockout littermates for each model group, confirming that the knockout met the requirements of our study (Fig. 2A, B). Results of H&E and PAS staining showed that the pathological injury and inflammatory infiltration, especially in the bronchi, especially in the bronchi, was significantly alleviated in NPSR knockout mice in either asthma model (Fig. 2C, D). In asthma, bronchial inflammation is typically marked by an elevated number of exfoliated cells and secretory proteins in the alveolar lavage fluid, accompanied by eosinophil infiltration. Our results

indicate that NPSR^{-/-} mice subjected to OVA- and papain-induced asthma exhibited reduced protein levels, lower cell counts (Fig. 2E, F). Flow cytometry analysis revealed that NPSR deficiency resulted in a reduction in the percentage of eosinophils (CD11c⁻Siglec-F⁺) in OVA- and Papain-induced asthmatic mice (Fig. 2G, H). These data provided evidence that NPSR promoted inflammation and exacerbated asthma.

To characterize the effect of NPSR on asthma, we performed comparative transcriptome analysis using RNA-seq in lung tissues from NPSR knockout compared to WT mice subjected to OVA and papain induced asthma. As shown in the volcano plots, we screened 194 up-regulated and 223 down-regulated genes in the papain-induced mice, and 166 differential genes, of which 114 were up-regulated and 52 down-regulated in the OVA-induced mice (Fig. 3C, D). These differential genes include asthma-related genes such as CCL11 (C–C Motif Chemokine Ligand 11), H2-Oa (Histocompatibility 2, O Region Alpha), MS4A2 (Membrane Spanning 4-Domains A2), CD40LG (CD40 Ligand), H2-Eb2 (Histocompatibility 2, Class II Antigen E Beta 2), IL-4 (Interleukin-4), IL-13 (Interleukin-13), and others. The heatmap displayed the top 150 different genes (Fig. 3A, B). Genomic enrichment analysis (GSEA) showed that asthma pathway enrichment was significantly downregulated in NPSR knockout mice model compared to WT mice model (Fig. 3E), this further suggested the involvement of NPSR in regulating asthma.

We further examined the expression of airway asthmatic factors, founding that the mRNA level of IL-4, IL-5 (Interleukin 5), IL-13, MUC5AC, and TSLP in lung tissues were significantly reduced in NPSR deficient mice (Fig. 3F). In addition, in NPSR-deficient mice induced with OVA and papain, the levels of Th2 cytokines, including IL-4, IL-5, and IL-13 (Fig. 3G), as well as serum IgE production (Fig. 3H), were significantly reduced in the BALF, as determined by ELISA, compared to non-knockout mice. These results suggested that NPSR promoted

(See figure on next page.)

Fig. 1 NPSR is upregulated in the lung tissue of asthmatic mice. **A** Diagrammatic illustration of the OVA-induced asthma mouse model. Mice were sensitized with 75 µg of OVA + alum adjuvant by intraperitoneal injection on days 0 and 10 of the experiment. On days 21, 22, and 23, intratracheal administration of OVA (50 µg) dissolved in PBS was used to challenge model mice and then sacrificed on day 25. Schematic protocol of the Papain-induced asthma model. Mice were sensitized with 40 µg of Papain administered endotracheally on days 0, 1, and 2, and then sacrificed on day 7. **B** H&E staining of lung tissue from wild-type mice treated with different drugs. **C, D** Protein levels and cell counts in alveolar lavage fluid. **E** Relative mRNA expression levels of inflammatory factors in lung tissue. **F, G** Immunoblot analysis of NPSR protein expression in lung tissues from OVA-induced mice and Papain-induced mice and quantified using Image J software. **H, I** The mRNA level of NPS and NPSR in lung tissues from OVA-induced mice and Papain-induced mice was quantified using qRT-PCR. **J** Immunohistochemical staining reveals NPSR expression in lung tissues of asthmatic mice. **K** Immunofluorescence analysis of NPSR expression in the lung tissues. NPSR (red), epithelial cells marker Ep-CAM (green), cell nucleus (DAPI, blue), merge (NPSR + Ep-CAM + DAPI); scale bars: 100 µm. Analysis of human primary airway epithelial cells stimulated with (n=4) and without IL-13 (n=4) in the GEO database GSE37693: (L) RNA volcano plots, (M) Violin plots. Data are shown as mean ± SEM. n = 5–7 mice for each group, * p < 0.05, ** p < 0.01, *** p < 0.001, n.s., non-significant difference

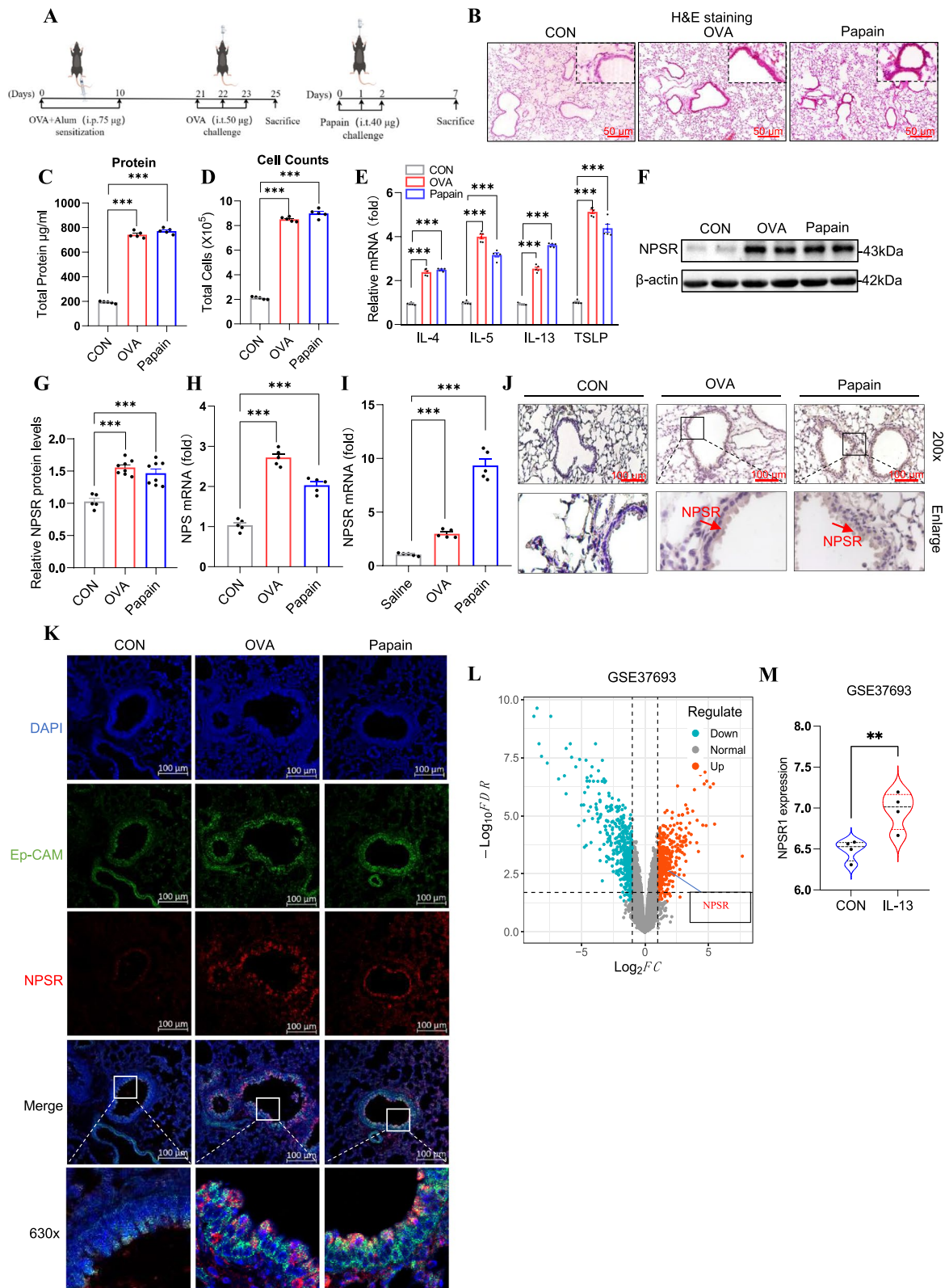


Fig. 1 (See legend on previous page.)

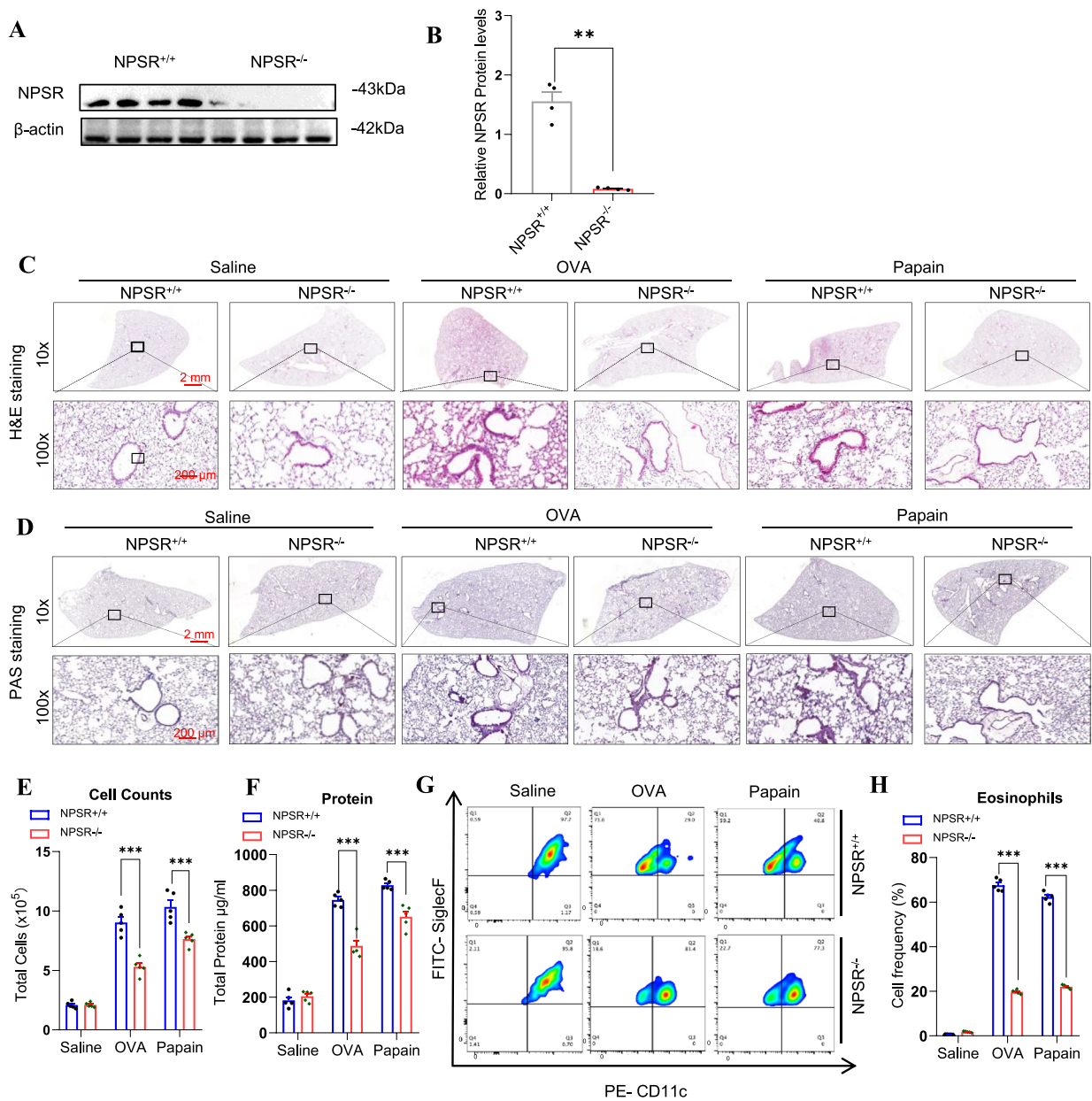


Fig. 2 NPSR knockout relieves asthma and airway inflammation. **A, B** Relative protein and mRNA expression levels of NPSR. **C, D** Histological analysis of H&E or PAS-stained lung sections from lung tissues of OVA- or papain-induced NPSR knockout and non-knockout mice. **E** Cell counts from BALF cells of papain- or OVA-induced asthmatic mice. **F** Detection of protein content of BALF from papain or OVA-induced asthmatic mice. **G** BALF cells from papain-induced asthma mice were stained with PE-CD11c and FITC-Siglec-F and evaluated by flow cytometry. Eosinophils (Eos, CD11c-Siglec-F+) were identified. **H** Percentage of eosinophils in BALF. Data are shown as mean \pm SEM. n = 5–7 mice for each group, * p < 0.05, ** p < 0.01, *** p < 0.001. n.s, non-significant difference

the inflammatory response and led to exacerbated asthma.

Activation of NPSR affects airway inflammation by modulating autophagy

To investigate the mechanism of NPS-NPSR system in regulating asthma, we performed the GO and KEGG

analysis for the transcriptome sequencing data, finding that inflammatory cytokine and autophagy pathways were enriched (Fig. 4A–D). In addition, protein network interactions indicated that NPSR and autophagy were closely linked (Fig. 4E). Therefore, we measured the expression of autophagy-related genes in lung tissues from different groups of mice. The results showed that

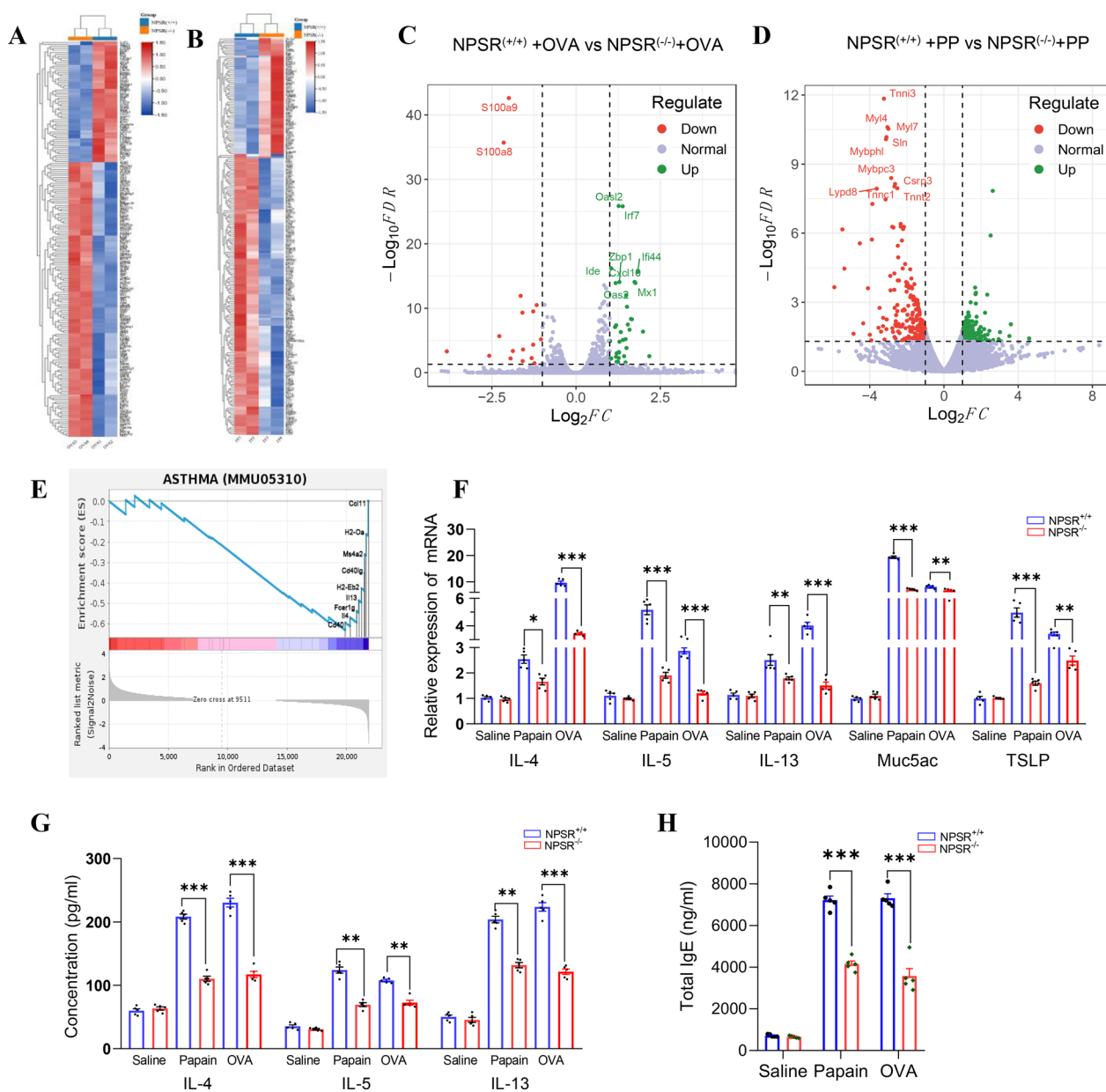


Fig. 3 NPSR knockdown reduces asthma-associated inflammatory factor release. **A, B** Heatmaps of OVA or papain-induced differential gene expression in NPSR knockout and non-knockout mice. **C, D** Volcano plots of NPSR knockout and non-knockout asthmatic mice induced with papain or OVA. **E** The GSEA of NPSR knockout and non-knockout asthmatic mice induced with OVA. **F** The mRNA level of IL-4, IL-5, IL-13, TSLP and muc5ac in lung tissues of NPSR knockout and non-knockout asthmatic mice induced with OVA or Papain was quantified using qRT-PCR. **G** Elisa for IL-4, IL-5, and IL-13 in BALF. **H** Elisa for serum IgE. Data are shown as mean ± SEM. n=5–7 mice for each group, * p < 0.05, ** p < 0.01, *** p < 0.001. n.s, non-significant difference

ATG5, LC3II, and Beclin-1 were significantly increased in OVA and papain-induced mice, while NPSR knockout inhibited the upregulation of ATG5, LC3II, and Beclin-1. Meanwhile, P62 was decreased in OVA and papain-induced mice, and NPSR knockout restored their expression (Fig. 4F–I). These results suggested that NPSR may promote asthma via regulating the autophagy process.

NPS-NPSR promotes autophagy in bronchial epithelial cells during asthma process

Given that NPSR positive-expression was mainly localized on the bronchial epithelial cells as shown in Fig. 1 F, we further investigated the autophagy change in bronchial epithelial cells by immunofluorescence analysis against LC3 and Ep-CAM, the data showed that LC3

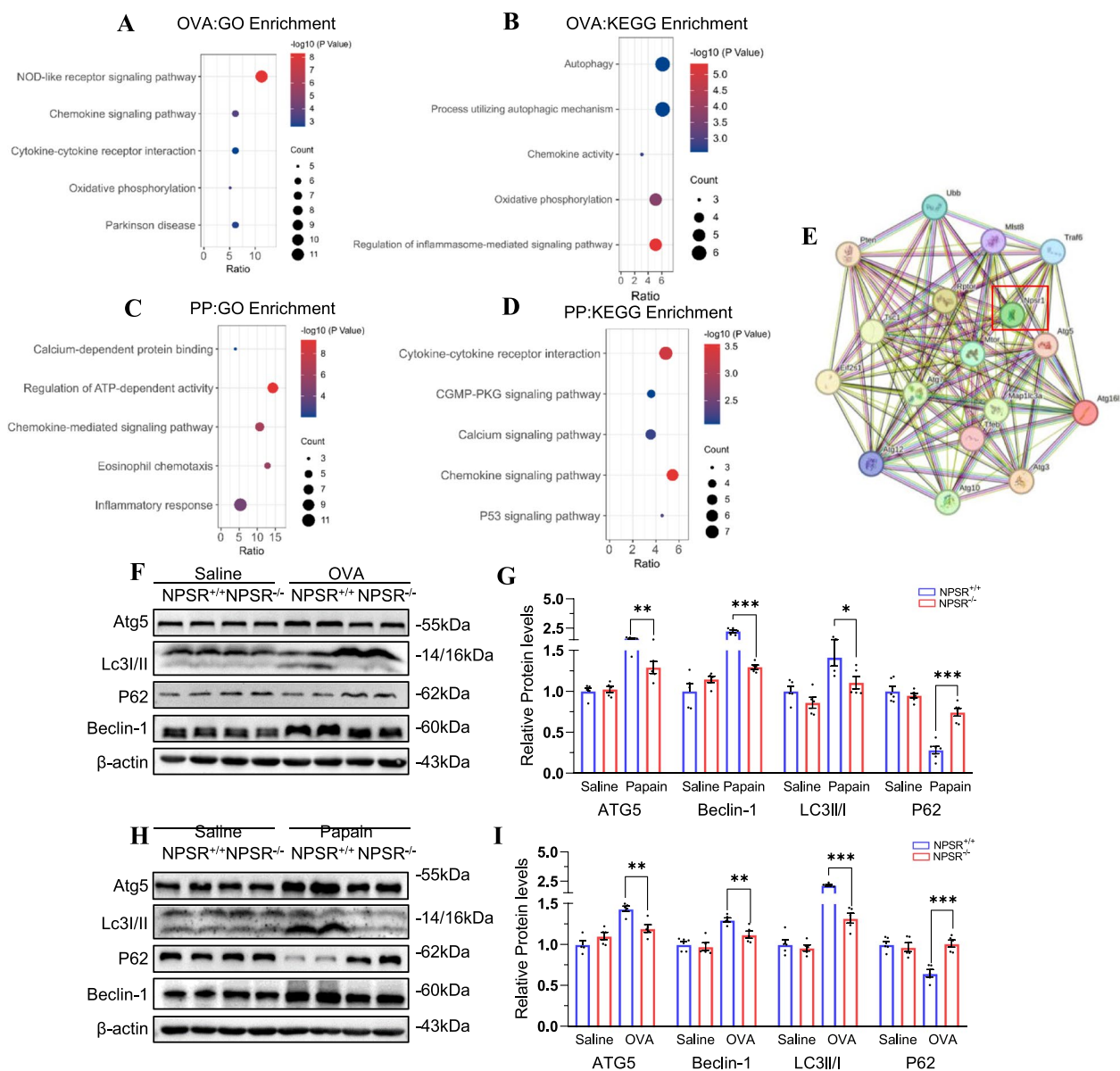


Fig. 4 NSPR knockdown attenuates autophagy in lung tissue. **A, B** The GO and KEGG enrichment analysis of differentially expressed genes in NPSR knockout and non-knockout asthmatic mice induced with OVA. **C, D** The GO and KEGG enrichment analysis of differentially expressed genes in NPSR knockout and non-knockout asthmatic mice induced with papain. **E** PPI network diagram of NPSR and autophagy-related genes. **F-I** The Protein immunoblot analysis of ATG5, Lc3b, P62, Beclin-1 and beta-actin in lung tissues of OVA and papain-induced NPSR^{+/+} and NPSR^{-/-} mice and quantified using ImageJ software. Data are shown as mean ± SEM. n = 5–7 mice for each group, * p < 0.05, ** p < 0.01, *** p < 0.001. n.s., non-significant difference

expression in bronchial epithelial cells was markedly downregulated in NPSR knockout mice model compared with WT mice model (Fig. 5D, E, G). Therefore, we treated the bronchial epithelial cell line (Beas-2b cells) with OVA followed by the administration of saline, exogenous NPS or NPSR blocker SHA68 respectively in vitro. As shown in Fig. 5A and B, OVA treatment promoted the level of autophagy related protein including Atg5,

LC3II, and Beclin-1, which were further upregulated by exogenous NPS treatment, but downregulated by challenge of NPSR blocker SHA68. Meanwhile, P62 expression was reduced by OVA administration and further downregulated followed by exogenous NPS treatment, but upregulated by SHA68 treatment (Fig. 5A, B). Similarly, the immunofluorescence staining also revealed that NPS exacerbated the expression level of LC3, while NPSR

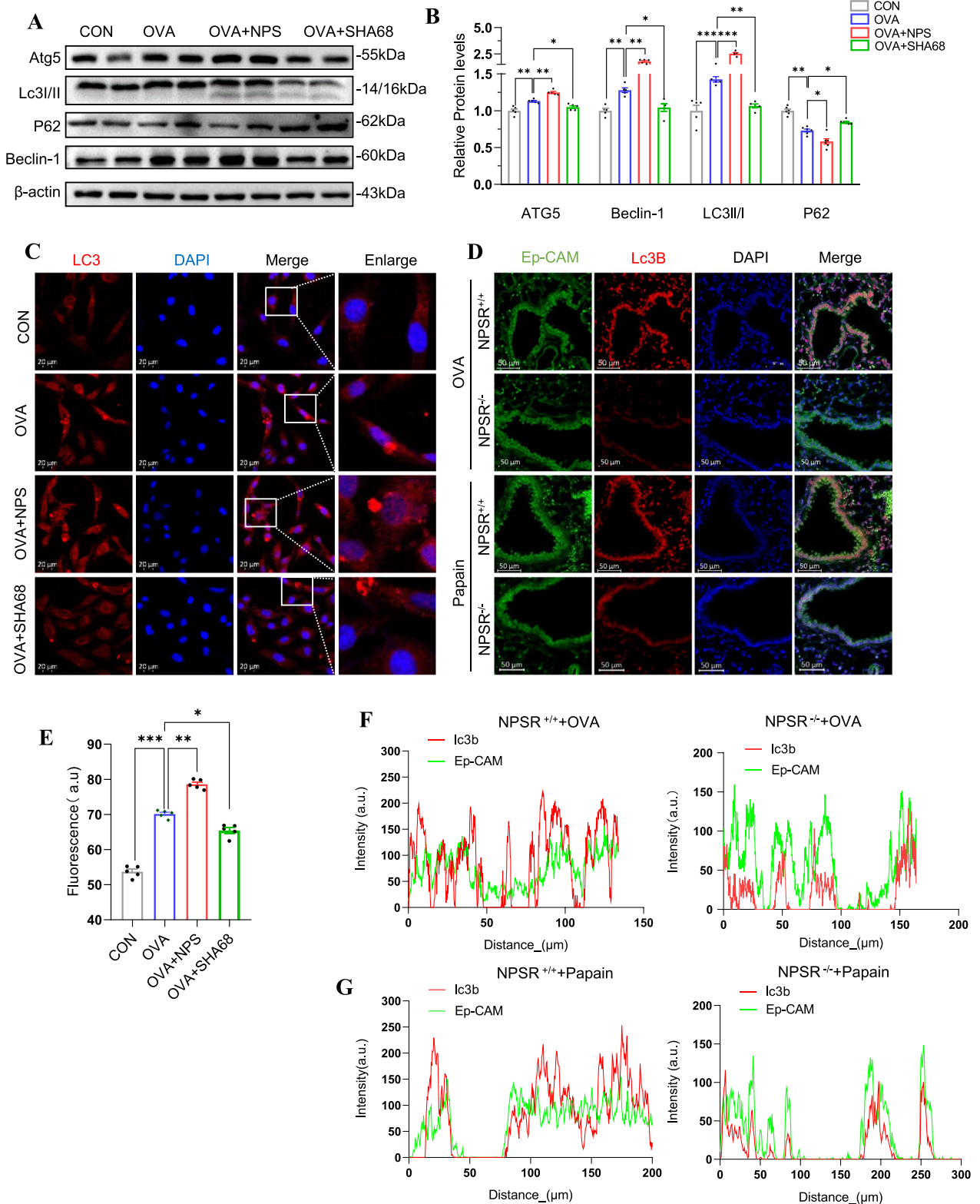


Fig. 5 Activation of NSPR exacerbates autophagy in bronchial epithelial cells. **A, B** The Protein immunoblot analysis of ATG5, LC3 I/II, P62, Beclin-1, and beta-actin and quantified using Image J software. **C, E** Immunofluorescence reveals the labeling of LC3 and is quantified using ImageJ software. **D–G** Immunofluorescence reveals labeling of Ep-CAM and LC3 I/II in lung tissue of asthmatic mice and quantified using Image J software. Data are shown as mean ± SEM. n = 5–7 mice for each group, * p < 0.05, ** p < 0.01, *** p < 0.001. n.s., non-significant difference

blocker SHA68 significantly blocked the upregulation of OVA-induced and compared with the control group (Fig. 5C, E).

TFEB was activated in NPS-NPSR controlled Beas-2b cells

Transcription factor EB (TFEB) is a major regulator of autophagy process and was shown to associate in asthma disease [32–37]. Here we investigated whether NPS regulates autophagy via activating TFEB in Beas-2b cells. We treated Beas-2b cells with NPS and found that the mRNA levels of TFEB was significantly increased in Beas-2b cells (Fig. 6A). Moreover, OVA treatment could increase the protein expression and nuclear transport, which was

exacerbated by exogenous NPS challenge and blocked by SHA68 challenge (Fig. 6B–E). Expectedly, the confocal microscopy also showed more nuclear translocations of TFEB in OVA plus NPS treated cells but less nuclear translocations in OVA plus SHA68 treated cells (Fig. 6F, G).

TFEB silence reduces NPS-induced autophagy and release of asthmatic cytokines in Beas-2b cells

To further confirm the role of TFEB in NPS-NPSR regulated autophagy during asthma process, we firstly conducted TFEB siRNA and control siRNA, and transfected them to evaluate the knockdown efficiency. The

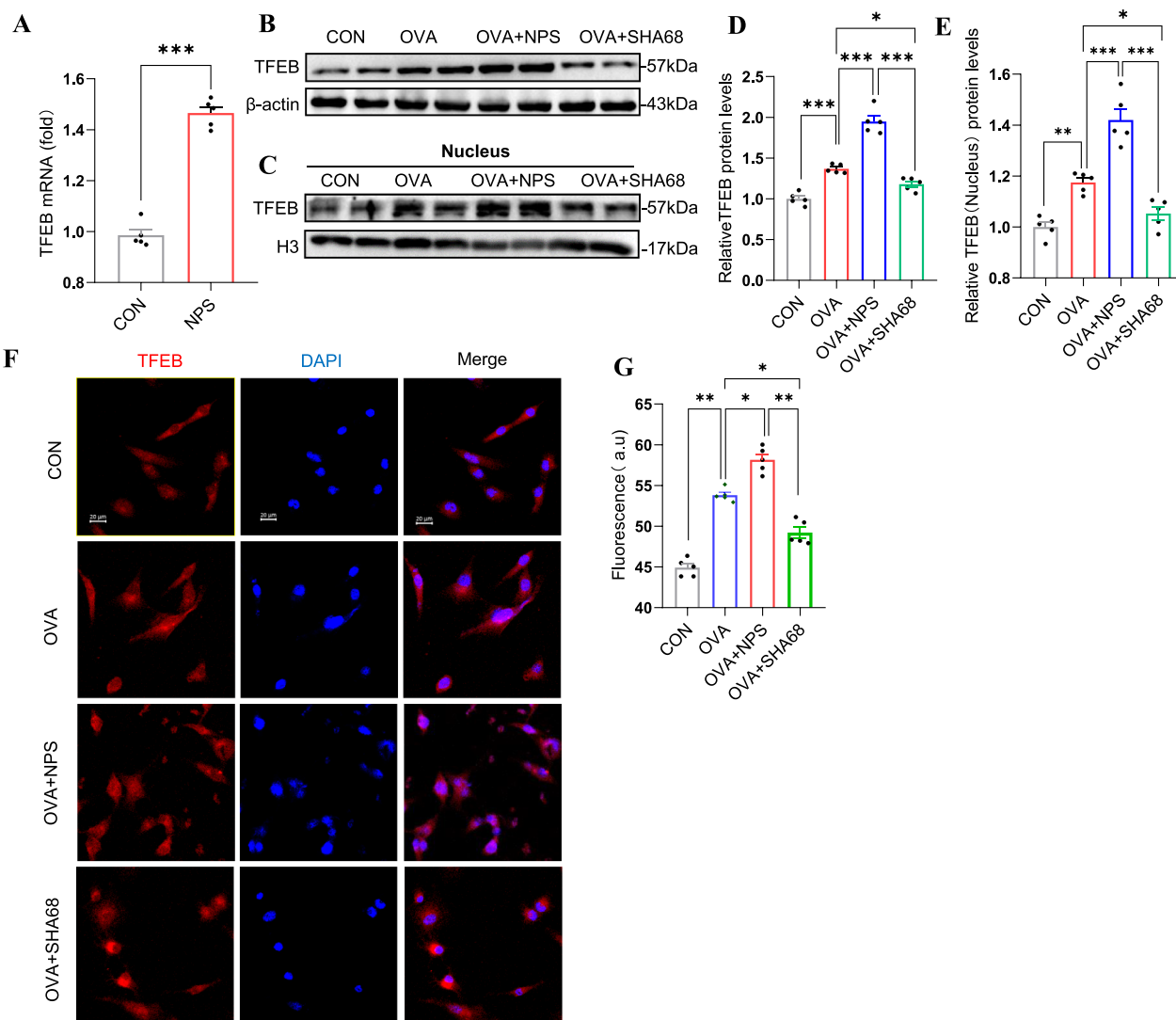


Fig. 6 Activation of NPSR can cause translocation of TFEB into the nucleus. **A** The mRNA level of TFEB was detected with qRT-PCR. **B–E** The Protein immunoblot analysis of total and intranuclear TFEB in Beas-2b cells and quantified using Image J software. **F, G** Immunofluorescence reveals labeling of TFEB and quantified using Image J software. Data are shown as mean ± SEM. n = 5–7 for each group, * p < 0.05, ** p < 0.01, *** p < 0.001. n.s., non-significant difference

RT-qPCR and immunoblotting detection showed mRNA and protein expression of TFEB was significantly silenced in Beas-2b cells (Fig. 7A–C). Importantly, we observed that silence of TFEB could markedly reduce the over-expression of autophagy-related genes including Atg5, Beclin-1, and LC3b by NPS stimulation in Beas-2b cells (Fig. 7E, F). Similarly, confocal microscopy showed that transfection of TFEB-siRNA resulted in diminished LC3 localization signals in NPS-treated Beas-2b cells (Fig. 7D, G). Subsequently, we examined the level of asthmatic factors IL-25, IL-33, and TSLP in Beas-2b cells with different treatments. The results showed that silence of TFEB significantly downregulated the release of IL-25, IL-33, and TSLP by NPS induction (Fig. 7H). We continued to examine the autophagy and asthmatic factor release in TFEB knockdown cells with control, OVA, OVA+NPS, or OVA+SHA68 treatment. The results demonstrated that siTFEB effectively reduced OVA-induced autophagy in BEAS-2B cells. This was evidenced by the stabilization of protein levels for Beclin-1, ATG5, and P62 following siTFEB treatment, as well as the inhibition of LC3 I to LC3 II conversion (Fig. 7I, J). Interestingly, the levels of IL-25, IL-33, and TSLP remained slightly elevated in the OVA+siTFEB group compared to the CON+siTFEB group, suggesting that the pro-inflammatory effects of OVA on BEAS-2B cells may also be mediated through alternative mechanisms. Moreover, there were no significant differences in the levels of inflammatory factors among the OVA+siTFEB, OVA+NPS+siTFEB, and OVA+SHA68+siTFEB groups (Fig. 7K). These findings underscore the critical role of TFEB as a downstream effector in the OVA-NPS-NPSR signaling axis contributing to inflammation. Taken together, our results validate that NPS contributed to autophagy via activating TFEB pathway in Beas-2b cells.

Prkcg mediated TFEB pathway involves in NPS-NPSR regulated asthma

Upon further analysis of the transcriptome sequencing data, we found that 10 of the 407 differential genes overlapped in papain-induced asthma model and OVA-induced asthma model. Wherein, protein kinaseγ(Prkcg) is significantly upregulated in both asthma models (Fig. 8A). The in vitro experimental results showed

the mRNA and protein level of Prkcg was significantly decreased by exogenous NPS treatment but increased by SHA68 treatment in Beas-2b cells (Fig. 8B–D). In vivo, the mRNA and protein levels of Prkcg was higher, accompanied with lower expression of TFEB in the lung tissues of NPSR knockout mice subjected to both OVA and papain induced asthma compared with that of WT asthma models (Fig. 8E–G).

Discussion

Asthma is a refractory respiratory disease with limited treatment options. Current therapeutic agents such as inhaled cortisol, long-acting beta-agonists (LABAs), anti-histamines, and leukotriene modulators focus on symptomatic relief rather than cure [2, 38]. Therefore, in-depth exploration of the pathogenesis of asthma is important to discover new therapeutic targets for asthma.

Neuropeptide S (NPS) is a bioactive 20 amino acid peptide that activates the orphan G-protein coupled receptor NPSR. It has been reported that the NPS-NPSR system is not only expressed in the central nervous system but also distributed in peripheral tissues to control various behavioral responses and diseases [20, 21, 25]. NPSR was uncovered to be a human asthma susceptibility gene screened by genomics [23, 25], and a higher mRNA level of this gene was also observed in asthma patients from the GEO profiles. These studies have suggested an association between NPS-NPSR system and asthma, but still with unclear understanding. In the present study, we demonstrated that the upregulation of NPS-NPSR contributed to asthma. Mice with established asthma had increased NPS and NPSR expression in lung tissues compared with healthy mice. NPSR^{-/-} mice exhibited significantly alleviated asthma and reduced inflammation in the lungs compared with WT mice subjected to ovalbumin (OVA) and papain-induced asthma. In vitro studies have suggested that NPS-NPSR prompted asthmatic inflammation through upregulation of TFEB-mediated autophagy in bronchial epithelial cells. These data confirmed our hypothesis in murine asthma models and in vitro.

The characteristics of airway epithelial cells, due to their direct contact with allergens, dictate that they are both mediators and targets of inflammation [39].

(See figure on next page.)

Fig. 7 TFEB silencing reduces NPS-induced autophagy levels in Beas-2b cells to attenuate inflammation. **A, B** The Protein immunoblot analysis of TFEB and quantified using Image J software. **C** The mRNA level of TFEB was detected with qRT-PCR. **D, G** Immunofluorescence reveals labeling of LC3 and quantified using Image J software. **E, F** The Protein immunoblot analysis of ATG5, LC3 I/II, and TFEB and quantified using Image J software. **H** The mRNA levels of IL25, IL33, TSLP were detected with qRT-PCR. **I, J** The Protein immunoblot analysis of TFEB and quantified using Image J software. **K** The mRNA levels of IL25, IL33, TSLP were detected with qRT-PCR. Data are shown as mean ± SEM. n = 5–7 mice for each group, * p < 0.05, ** p < 0.01, *** p < 0.001. n.s, non-significant difference

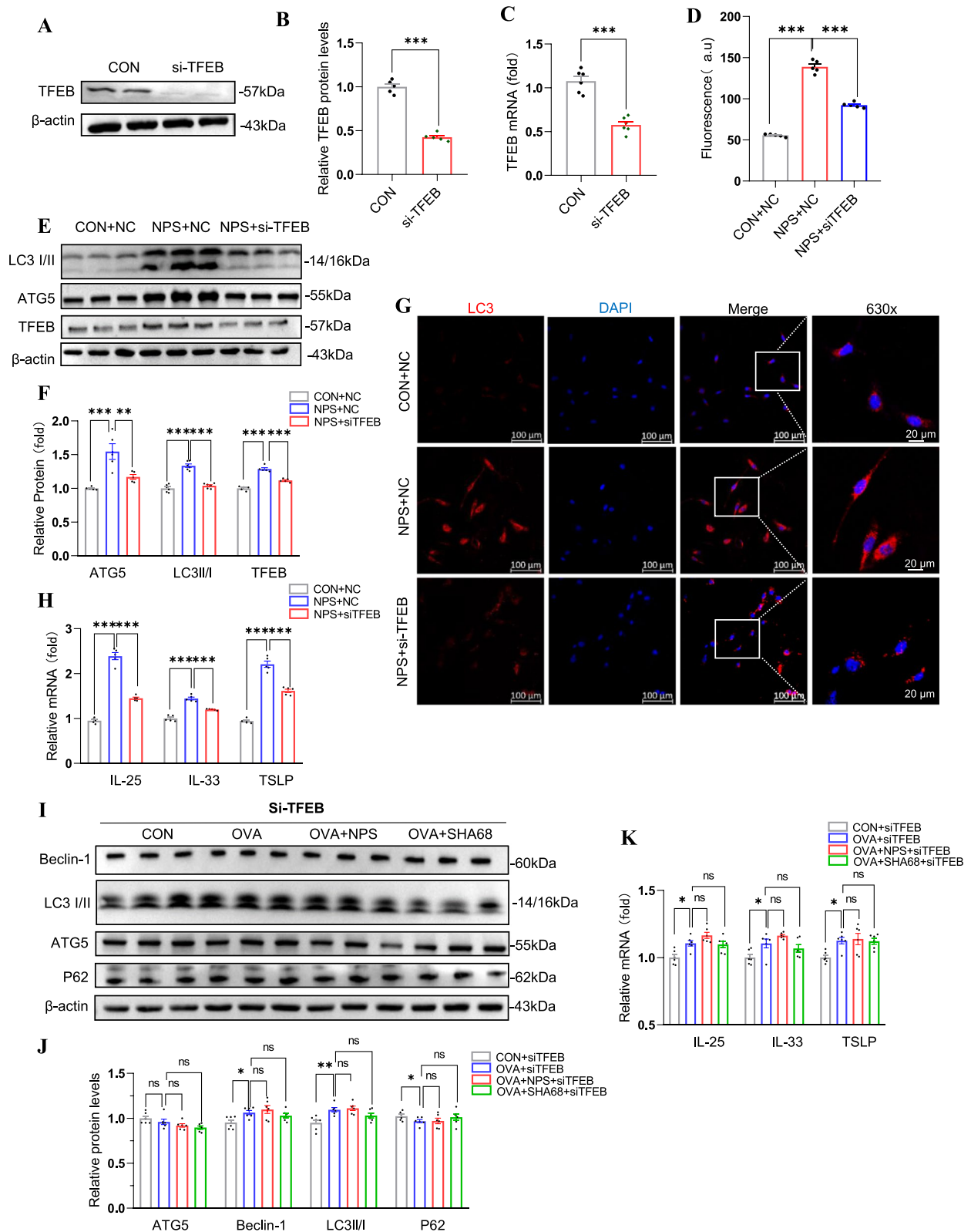


Fig. 7 (See legend on previous page.)

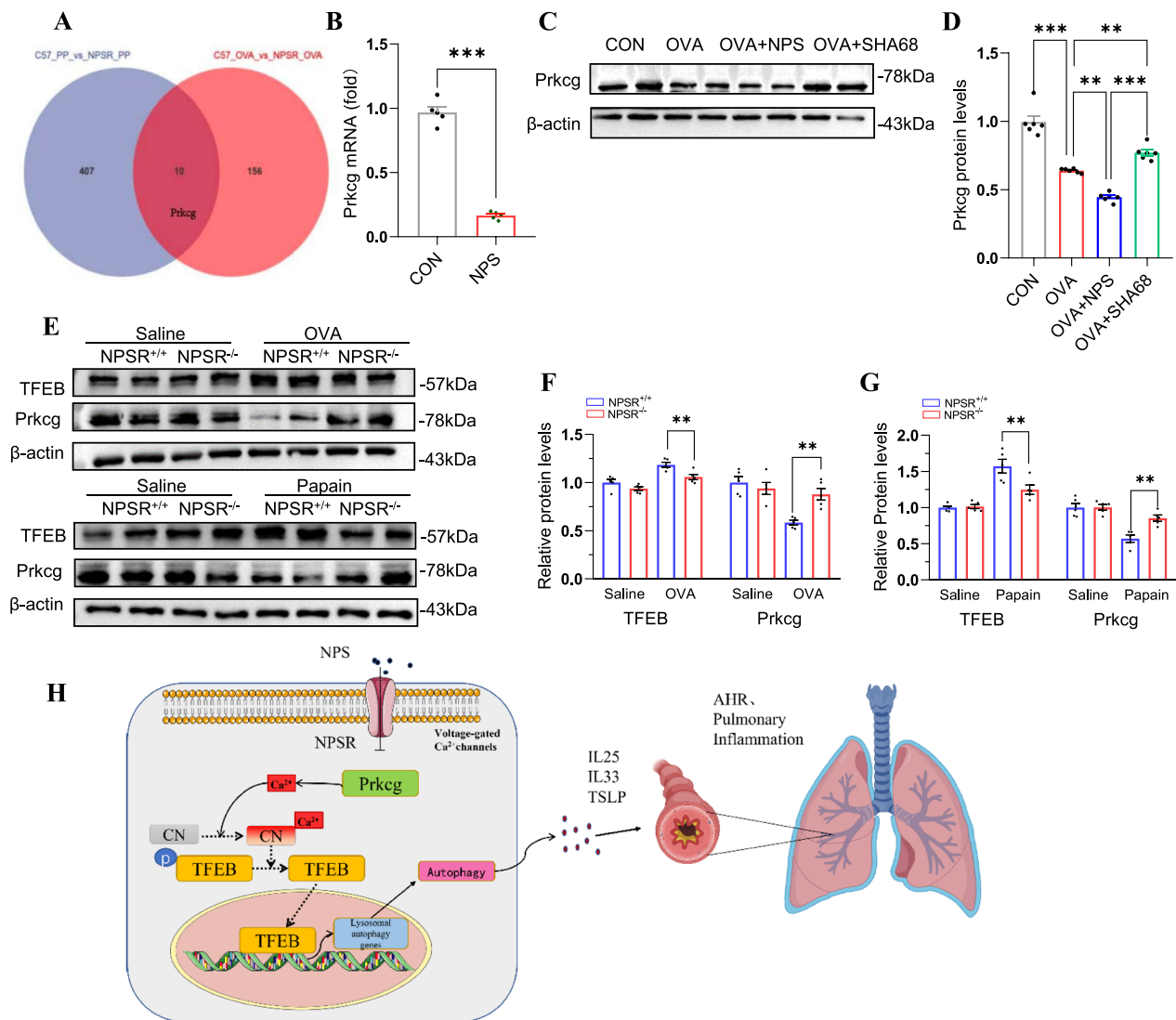


Fig. 8 NPS-NPSR may affect TFEB translocation into the nucleus by inhibiting Prkcg. **A** Venn diagram of common differential genes in OVA-induced NPSR knockout and non-knockout asthma mice and Papain-induced asthma mice. **B** The mRNA level of Prkcg was detected with qRT-PCR. **C, D** The Protein immunoblot analysis of Prkcg and quantified using Image J software. **E-G** The Protein immunoblot analysis of Prkcg and TFEB in lung tissues from OVA-induced mice and Papain-induced mice was quantified using Image J software. **H** A schematic diagram showing TFEB-dependent regulation of autophagy upon NPSR activation. Data are shown as mean \pm SEM. $n = 5-7$ mice for each group, * $p < 0.05$, ** $p < 0.01$, *** $p < 0.001$. n.s., non-significant difference

Previous studies have shown that the airway epithelium initiates an immune response against pathogen attack through multimodal recognition receptors [40]. At the same time, airway epithelial cells can also secrete pro-inflammatory and anti-inflammatory factors to regulate the inflammatory response. It has been found that dysregulation of the epithelial-mesenchymal transition in response to chronic allergenic stimuli often leads to amplified inflammatory responses, abnormal airway remodeling, and incomplete tissue repair, thereby exacerbating asthma [39, 40]. In addition, the researchers

found that airway epithelial cells are the primary target of inflammatory attack by T cells and eosinophils and that bronchial epithelial cells can also phagocytose apoptotic eosinophils in a specific receptor-mediated manner [41, 42]. Additionally, airway epithelial cells can secrete various inflammatory mediators that drive the development of asthma [43-46]. Thus, dysregulation of the epithelial cells often leads to amplified inflammation and abnormal airway remodeling, thereby exacerbating asthma [43-46]. This study clarifies for the first time that the increased expression of

NPS-NPSR was mainly distributed in bronchial epithelial cells, KEGG analysis revealed enrichment in inflammatory cytokines and asthmatic genes, suggesting the function of NPS-NPSR in the bronchial epithelial cells on prompting asthma. Interestingly, an important cellular mechanism for homeostasis autophagy was also enriched in the KEGG analysis, showing significant expression differences between NPSR^{-/-} and WT mice subjected to OVA challenge. Aberrant autophagy has been shown to play a vital role in asthma [13, 15]. Humans and mice with asthma displayed higher levels of autophagy compared to normal control [47, 48], and suppression of autophagy by chloroquine significantly attenuated airway inflammation, mucus, and collagen production during asthmatic process [14–16, 19, 34]. Here we revealed that OVA and papain induced the expression of autophagy-related genes LC3II, ATG5, and Beclin-1 with the downregulated level of SQSTM1 (p62) in vivo, NPSR knockout restored the upregulation of autophagy in bronchial epithelial cells of asthma models. The in vitro experimental data further showed that NPS-NPSR contributed to autophagy using exogenous NPS and pharmacological blockers of NPSR. Thus, the in vivo and in vitro experimental results provided evidence that NPS-NPSR aggravated asthma via promoting autophagy in bronchial epithelial cells.

Transcription factor EB (TFEB) is one of the major transcriptional regulators of autophagy that promotes autophagosome formation, lysosomal biosynthesis, and expression of genes required for lysosomal function [32–35, 49]. Our data showed that the expression and nuclear transport of TFEB was markedly increased by OVA or OVA plus NPS treatment, but decreased by NPSR blocker SHA68 in bronchial epithelial cells. To further determine the effect of NPS-NPSR on the activation of TFEB, we directly stimulated the cells with NPS. As expected, TFEB-involved autophagy was significantly upregulated, and TFEB silence blocked the function of NPS on autophagy in bronchial epithelial cells, resulting in less secretion of asthmatic cytokines including IL-25, IL-33, and TSLP. In addition, the RNA-seq analysis showed elevated Prkcg expression in OVA and papain-induced mice models was down in NPSR knockout mice. Prkcg (PKC- γ) is an isoform of protein kinase C that is involved in various cellular processes. Previous studies showed that Prkcg can interact with the protein phosphatase 2B [50], a calmodulin neural phosphatase that has been identified to regulate TFEB dephosphorylation and nuclear translocation [36, 37]. Therefore, the activation of TFEB by NPS-NPSR is likely via inhibition of Prkcg in OVA and papain-induced mice models and Beas-2b cells.

In conclusion, we showed that NPS-NPSR regulated autophagy via TFEB in airway epithelial cells, which contributed to OVA and papain-induced asthma, providing a potential target for the therapeutic strategies of asthma.

Abbreviations

BALF	Bronchoalveolar lavage fluid
Eos	Eosinophils
GSEA	Genomic enrichment analysis
GWAS	Genome-wide association study
H&E	Hematoxylin and eosin staining
LABAs	Long-acting beta-agonists
NPS	Neuropeptide S
NPSR1	Neuropeptide S receptor 1
OVA	Ovalbumin
PAS	Periodic acid-Schiff stain
Prkcg/ PKC- γ	Protein kinase γ
siTFEB	Small interfering RNA against TFEB
SNPs	Single nucleotide polymorphisms

Acknowledgements

Not applicable.

Author contributions

Zhixu Wang and Yunjuan Nie designed the experiments; Zhixu Wang, Li Xu, Jiao Li, Xiaorun Zhai, Xiangcen Liu, Tingting Mei, Aijuan Sun and Yinghua Xuan performed the experiments and analyzed the data; Zhixu Wang, Peng Zhao, Aijuan Sun, Gen Yan and Yunjuan Nie prepared the manuscript.

Funding

This study was supported by the National Natural Science Foundation of China (81800065), the Natural Science Foundation of Jiangsu Province (BK20180616), the National Postdoctoral Science Foundation of China (2021M691292), and the Postdoctoral Science Foundation of Jiangsu Province (2020Z132).

Availability of data and materials

No datasets were generated or analysed during the current study.

Declarations

Ethics approval and consent to participate

The JNU Animal Care approved procedures involving mice and Use Teaching Committee (JN. No20230830m0880315 [350], approval date 8/30/2023).

Consent for publication

Not applicable.

Competing interests

The authors declare no competing interests.

Received: 18 November 2024 Accepted: 27 January 2025

Published online: 10 February 2025

References

- Adhikary PP, Tan Z, Page BDG, Hedtrich S. TSLP as druggable target—a silver-lining for atopic diseases? *Pharmacol Ther.* 2021;217: 107648.
- Castillo JR, Peters SP, Busse WW. Asthma exacerbations: pathogenesis, prevention, and treatment. *J Allergy Clin Immunol Pract.* 2017;5:918–27.
- Papi A, Brightling C, Pedersen SE, Reddel HK. Asthma. *Lancet.* 2018;391:783–800.
- Hellings PW, Steelant B. Epithelial barriers in allergy and asthma. *J Allergy Clin Immunol.* 2020;145:1499–509.

5. Heijink IH, Kuchibhotla VNS, Roffel MP, Maes T, Knight DA, Sayers I, Nawijn MC. Epithelial cell dysfunction, a major driver of asthma development. *Allergy*. 2020;75:1902–17.
6. Golebski K, Röschmann KL, Toppila-Salmi S, Hammad H, Lambrecht BN, Renkonen R, Fokkens WJ, Van Druenen CM. The multi-faceted role of allergen exposure to the local airway mucosa. *Allergy*. 2013;68:152–60.
7. Georas SN, Rezaee F. Epithelial barrier function: at the front line of asthma immunology and allergic airway inflammation. *J Allergy Clin Immunol*. 2014;134:509–20.
8. Hewitt RJ, Lloyd CM. Regulation of immune responses by the airway epithelial cell landscape. *Nat Rev Immunol*. 2021;21:347–62.
9. Jakwerth CA, Ordovas-Montanes J, Blank S, Schmidt-Weber CB, Zissler UM. Role of respiratory epithelial cells in allergic diseases. *Cells*. 2022;11:1387.
10. Cao J, Ren G, Gong Y, Dong S, Yin Y, Zhang L. Bronchial epithelial cells release IL-6, CXCL1 and CXCL8 upon mast cell interaction. *Cytokine*. 2011;56:823–31.
11. Takizawa H. Bronchial epithelial cells in allergic reactions. *Curr Drug Targets Inflamm Allergy*. 2005;4:305–11.
12. Glick D, Barth S, Macleod KF. Autophagy: cellular and molecular mechanisms. *J Pathol*. 2010;221:3–12.
13. Kim KH, Lee M-S. Autophagy—a key player in cellular and body metabolism. *Nat Rev Endocrinol*. 2014;10:322–37.
14. Germic N, Hosseini A, Yousefi S, Karalov A, Simon H-U. Regulation of eosinophil functions by autophagy. *Semin Immunopathol*. 2021;43:347–62.
15. Zeki AA, Yeganeh B, Kenyon NJ, Post M, Ghavami S. Autophagy in airway diseases: a new frontier in human asthma? *Allergy*. 2016;71:5–14.
16. Theofani E, Xanthou G. Autophagy: a friend or foe in allergic asthma? *Int J Mol Sci*. 2021;22:6314.
17. Liu J-N, Suh D-H, Trinh HKT, Chwae Y-J, Park H-S, Shin YS. The role of autophagy in allergic inflammation: a new target for severe asthma. *Exp Mol Med*. 2016;48:e243–e243.
18. Dickinson JD, Alevy Y, Malvin NP, Patel KK, Gunsten SP, Holtzman MJ, Stapenbeck TS, Brody SL. IL13 activates autophagy to regulate secretion in airway epithelial cells. *Autophagy*. 2016;12:397–409.
19. Dickinson JD, Sweeter JM, Warren KJ, Ahmad IM, De Deken X, Zimmerman MC, Brody SL. Autophagy regulates DUOX1 localization and superoxide production in airway epithelial cells during chronic IL-13 stimulation. *Redox Biol*. 2018;14:272–84.
20. D'Amato M, Bruce S, Bresso F, Zucchelli M, Ezer S, Pulkkinen V, Lindgren C, Astegiano M, Rizzetto M, Gionchetti P, et al. Neuropeptide S receptor 1 gene polymorphism is associated with susceptibility to inflammatory bowel disease. *Gastroenterology*. 2007;133:808–17.
21. Kushikata T, Hirota K, Saito J, Takekawa D. Roles of neuropeptide S in anesthesia, analgesia, and sleep. *Pharmaceuticals*. 2021;14:483.
22. Bossé Y, Hudson TJ. Toward a comprehensive set of asthma susceptibility genes. *Annu Rev Med*. 2007;58:171–84.
23. Couzin J. Two new asthma genes. *Uncovered Sci*. 2004;304:185–7.
24. Castro-Giner F, de Cid R, Gonzalez JR, Jarvis D, Heinrich J, Janson C, Omenaas ER, Matheson MC, Pin I, Anto JM, et al. Positionally cloned genes and age-specific effects in asthma and atopy: an international population-based cohort study (ECRHS). *Thorax*. 2009;65:124–31.
25. Hersh CP, Raby BA, Soto-Quirós ME, Murphy AJ, Avila L, Lasky-Su J, Sylvia JS, Klanderman BJ, Lange C, Weiss ST, Celedón JC. Comprehensive testing of positionally cloned asthma genes in two populations. *Am J Respir Crit Care Med*. 2007;176:849–57.
26. Pulkkinen V, Majuri ML, Wang G, Holopainen P, Obase Y, Vendelin J, Wolff H, Ryttilä P, Laitinen LA, Haahtela T, et al. Neuropeptide S and G protein-coupled receptor 154 modulate macrophage immune responses. *Hum Mol Genet*. 2006;15:1667–79.
27. Zhang ZR, Tao YX. Physiology, pharmacology, and pathophysiology of neuropeptide S receptor. *Prog Mol Biol Transl Sci*. 2019;161:125–48.
28. Song Y, Wu Y, Li X, Shen Y, Ding Y, Zhu H, Liu F, Yu K, Sun L, Qian F. Protostemonine attenuates alternatively activated macrophage and DRA-induced asthmatic inflammation. *Biochem Pharmacol*. 2018;155:198–206.
29. Zhang H, Wei R, Yang X, Xu L, Jiang H, Li M, Jiang H, Zhang H, Chen Z, Qian F, Sun L. AMFR drives allergic asthma development by promoting alveolar macrophage-derived GM-CSF production. *J Exp Med*. 2022;219: e20211828.
30. Morita H, Arae K, Unno H, Miyauchi K, Toyama S, Nambu A, Oboki K, Ohno T, Motomura K, Matsuda A, et al. An interleukin-33-mast cell-interleukin-2 axis suppresses papain-induced allergic inflammation by promoting regulatory T cell numbers. *Immunity*. 2015;43:175–86.
31. Wei W, Chen W, He N. HDAC4 induces the development of asthma by increasing Slug-upregulated CXCL12 expression through KLF5 deacetylation. *J Transl Med*. 2021;19:258.
32. Cortes CJ, La Spada AR. TFEB dysregulation as a driver of autophagy dysfunction in neurodegenerative disease: molecular mechanisms, cellular processes, and emerging therapeutic opportunities. *Neurobiol Dis*. 2019;122:83–93.
33. Jeong S-J, Stitham J, Evans TD, Zhang X, Rodriguez-Velez A, Yeh Y-S, Tao J, Takabatake K, Epelman S, Lodhi IJ, et al. Trehalose causes low-grade lysosomal stress to activate TFEB and the autophagy-lysosome biogenesis response. *Autophagy*. 2021;17:3740–52.
34. Nakamura S, Akayama S, Yoshimori T. Autophagy-independent function of lipidated LC3 essential for TFEB activation during the lysosomal damage responses. *Autophagy*. 2021;17:581–3.
35. Zhang W, Li X, Wang S, Chen Y, Liu H. Regulation of TFEB activity and its potential as a therapeutic target against kidney diseases. *Cell Death Discov*. 2020;6:32.
36. Chen H, Gong S, Zhang H, Chen Y, Liu Y, Hao J, Liu H, Li X. From the regulatory mechanism of TFEB to its therapeutic implications. *Cell Death Discov*. 2024;10:84.
37. Zhou W, Yan X, Zhai Y, Liu H, Guan L, Qiao Y, Jiang J, Peng L. Phyllygenin ameliorates nonalcoholic fatty liver disease via TFEB-mediated lysosome biogenesis and lipophagy. *Phytomedicine*. 2022;103: 154235.
38. Lommatzsch M, Virchow JC. Severe asthma. *Deutsches Ärzteblatt International*; 2014.
39. Banno A, Reddy AT, Lakshmi SP, Reddy RC. Bidirectional interaction of airway epithelial remodeling and inflammation in asthma. *Clin Sci (Lond)*. 2020;134:1063–79.
40. Liu C, Zhang X, Xiang Y, Qu X, Liu H, Liu C, Tan M, Jiang J, Qin X. Role of epithelial chemokines in the pathogenesis of airway inflammation in asthma (Review). *Mol Med Rep*. 2018;17:6935–41.
41. Walsh G, Sexton D, Blaylock M. Corticosteroids, eosinophils and bronchial epithelial cells: new insights into the resolution of inflammation in asthma. *J Endocrinol*. 2003;178:37–43.
42. Trautmann A, Schmid-Grendelmeier P, Kruger K, Cramer R, Akdis M, Akkaya A, Brocker EB, Blaser K, Akdis CA. T cells and eosinophils cooperate in the induction of bronchial epithelial cell apoptosis in asthma. *J Allergy Clin Immunol*. 2002;109:329–37.
43. Goulopoulou S, McCarthy CG, Webb RC. Toll-like receptors in the vascular system: sensing the dangers within. *Pharmacol Rev*. 2016;68:142–67.
44. Galowitz S, Chang C. Immunobiology of critical pediatric asthma. *Clin Rev Allergy Immunol*. 2015;48:84–96.
45. Mitchell PD, O'Byrne PM. Biologics and the lung: TSLP and other epithelial cell-derived cytokines in asthma. *Pharmacol Ther*. 2017;169:104–12.
46. Holgate ST, Davies DE, Lackie PM, Wilson SJ, Puddicombe SM, Lordan JL. Epithelial-mesenchymal interactions in the pathogenesis of asthma. *J Allergy Clin Immunol*. 2000;105:193–204.
47. Xia F, Deng C, Jiang Y, Qu Y, Deng J, Cai Z, Ding Y, Guo Z, Wang J. IL4 (interleukin 4) induces autophagy in B cells leading to exacerbated asthma. *Autophagy*. 2018;14:450–64.
48. Sachdeva K, Do DC, Zhang Y, Hu X, Chen J, Gao P. Environmental exposures and asthma development: autophagy, mitophagy, and cellular senescence. *Front Immunol*. 2019;10:2787.
49. Yang J, Zhang W, Zhang S, Iyaswamy A, Sun J, Wang J, Yang C. Novel insight into functions of transcription factor EB (TFEB) in Alzheimer's disease and Parkinson's disease. *Aging Dis*. 2023;14:652.
50. Aronowski J, Grotta JC, Strong R, Waxham MN. Interplay between the gamma isoform of PKC and calcineurin in regulation of vulnerability to focal cerebral ischemia. *J Cereb Blood Flow Metab*. 2000;20:343–9.

Publisher's Note

Springer Nature remains neutral with regard to jurisdictional claims in published maps and institutional affiliations.